Numerical simulation on coupling behavior of Terfenol-D rods

Le Sun, Xiaojing Zheng *

Department of Mechanics, Lanzhou University, 222 TianShui South Road, Lanzhou 730000, PR China

Abstract

Terfenol-D rods, as a kind of giant magnetostrictive materials, are often used as active elements of device for anti-vibration application due to its superior material properties. Their magneto-mechanical responses exhibited in many experiments are nonlinear and coupled. In order to have a good understanding on their coupling characters for accurate control, the numerical simulation on dynamic behavior of a Terfenol-D rod is conducted based on a nonlinear and coupling constitutive model proposed in this paper. The results show that the constitutive model can effectively describe some intrinsic coupling phenomena observed by experiments involving the maximum magnetostrictive strain of a Terfenol-D rod changing with pre-stresses and the corresponding dynamic responses show that the frequency and the amplification of the Terfenol-D rod change with magnetic bias field and pre-stresses, which are also consistent with experimental data and cannot be captured by previous constitutive model.
© 2005 Elsevier Ltd. All rights reserved.

Keywords: Terfenol-D; Constitutive relations; ΔE effect; Resonance frequency; Numerical simulation

1. Introduction

With the application of sensors and actuators, more and more researches focus on the dynamic behavior of smart materials and structures (Zhou and Miya, 1999; Zhou and Tzou, 2000; Pelinescu and Balachandran, 2001; Mahapatra et al., 2001). As an important actuator to control vibration, Terfenol-D actuator has many advantages in performance such as large displacement, fast response, simple driving, wide frequency range, good low frequency character and so on. Moreover, the large strain of Terfenol-D rods

---

* Corresponding author. Tel.: +86 931 891 1727; fax: +86 931 862 5576.
E-mail address: xjzheng@lzu.edu.cn (X. Zheng).

can be transformed to linear displacement or vibration easily. So, Terfenol-D rods based devices have often been used in active control, noise control and high precision micro-positioning devices etc. (Rodtlett et al., 2001). Jenner et al. (1994) studied a vibration control case of Terfenol-D actuator by two kinds of control strategy. Engdahl and Svensson (1988) suggested a dynamic simulation model and gave the results under the variation magnetic field by SANDYS. Kvarnsjö and Engdahl (1991a) gave a nonlinear 2-D transient model of Terfenol-D rods and then they Kvarnsjö and Engdahl (1991b) improved the transient model, which took the influence of eddy currents.

For the Terfenol-D actuator, it is important to study the coupled mechanics-magneto properties fully and exactly in operation, since the expectant operating range is generally obtained by applying a magnetic bias field and a mechanical pre-stress. However, the experimental results have exhibited that the couple behavior is notable and complicated for the magnetostrictive materials. Fig. 1 shows the experimental curves of magnetostrictive strain versus magnetic field for Terfenol-D rods under different compressive pre-stress (Butler, 1988). As seen in Fig. 1, the magnetostrictive strain increases with an increasing magnetic field for a given pre-stress. Also it can be found that magnetostrictive strain decreases with increasing compressive pre-stress under low or moderate field, however, it will increase with increasing compressive pre-stress under high field, i.e., the larger the compressive pre-stress, the larger is the maximum magnetostrictive strain which is called the reversal phenomenon in this paper. It can be explained that there is a hard direction of magnetization along the axis of a Terfenol-D rod when it is subjected to an axial compressive pre-stress. When applied field is low or moderate field, the magnetostrictive strain is smaller under larger compressive pre-stress since the corresponding field is too small to overcome stress anisotropy at the time. However, the saturation magnetostrictive strain of a Terfenol-D rod will increase with increasing compressive pre-stress under high field since stress anisotropy is entirely overcome when the applied magnetic field approaches saturation one.

The coupled mechanics-magneto properties are also exhibited in the response of magnetostrictive device. Fig. 2 shows the experimental curves of resonance frequency versus magnetic bias field for Terfenol-D actuator (Savage et al., 1975). As shown in Fig. 2, resonance frequency increases with increasing bias field, which is due to the ΔE effect, i.e., Young's modulus of a Terfenol-D rod changes nonlinearly with the stress and the magnetic field. The ΔE effect can mirror the achievable changes in resonant frequency since it is proportional to resonance frequency squared.
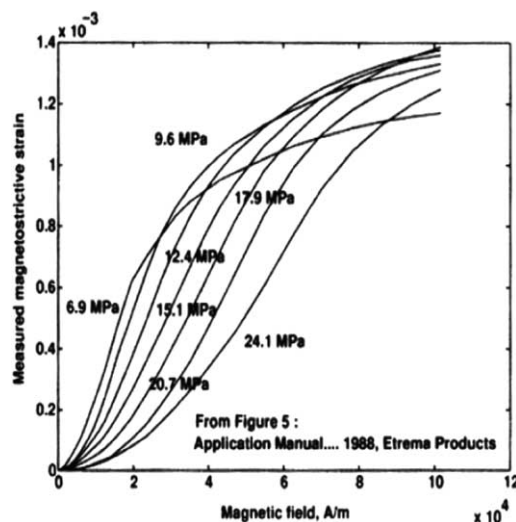

Fig. 1. The experimental curves of magnetostrictive strain versus magnetic field (Butler, 1988).
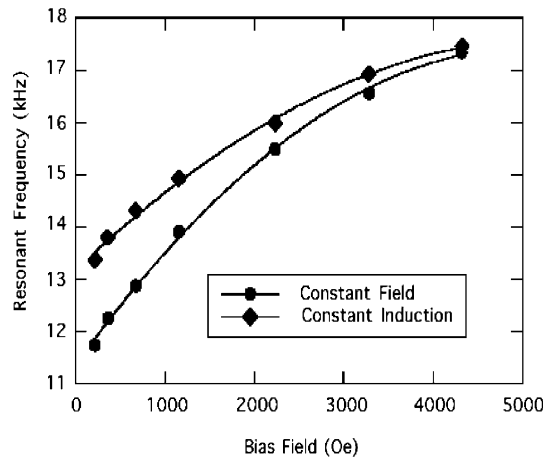
Fig. 2. The experimental curves of resonance frequency versus magnetic bias field (Savage et al., 1975).

Based on the above analysis, it can be noticed that the coupled mechanics-magneto properties are nonlinear for both material character and response of device. An accurate constitutive model of magnetostrictive materials should be suggested in order to increase control efficiency of Terfenol-D actuators and improve their designs. There were many previous nonlinear constitutive models for magnetostrictive materials, such as the standard square model, i.e., the SS model (Carman and Mitrovic, 1995), the hyperbolic tangent model, i.e., the HT model (Wan et al., 2003) and the model based on density of domain switching, i.e., the DDS model (Wan et al., 2003) as well as the model derived by Duenas et al. (1996) called the D–H model in the paper. By comparison with Moffet et al.'s (1991) experimental results, it is found that there are obvious deficiencies for these previous models. For example, the SS model can neither describe the saturation nor can it provide an accurate prediction for the low pre-stresses. Both the HT model and the DDS model can predict the saturation yet there are much errors in quantity, moreover, the two models cannot provide an accurate prediction for the high pre-stresses through all the range of magnetic field. The D–H model is found to be able to accurately predict magnetostrictive strain values in the region of the low and moderate magnetic fields for various pre-stress levels and also the saturation but it cannot describe the reversal phenomena shown in Fig. 1. (Detailed discussion is given later.)

In order to better describe the influence of magnetic bias field and pre-stress on magnetostrictive material and corresponding device, a new model is suggested in this paper. It can describe nonlinearity and coupled mechanics-magneto properties more effectively than the above model. The numerical results exhibit the fact that magnetostrictive strain curves predicted by the model are in good agreement with the experimental data given by Moffet et al. (1991) for various compressive pre-stresses and various magnetic field and it can simulate the reversal phenomena shown in Fig. 1. Furthermore, the new model can effectively describe the influence of the stress and the magnetic field on Young's modulus, i.e., the ΔE effect. Thus, the resonance frequency based on the model can be exhibited changing not only with pre-stress but also with the magnetic field just like the experiment shown in Fig. 2. Additionally, the resonance amplitude is found changing with the magnetic field too. Finally, the model can describe the ultraharmonic resonance phenomena of Terfenol-D actuator. All of these benefit from the advantage of the new model in accurately describing the nonlinearity of magnetostrictive material under high field.

For all of the above previous nonlinear constitutive models, only the D–H model can describe the coupled character preferably, in part 4 we will mostly give a comparison between the D–H model and the model suggested in this paper.

2. The establishment of constitutive model

The new model uses a Taylor series, expansion of the elastic Gibbs free energy function $G(\sigma, M)$ at the reference point $(\sigma, M) = (0,0)$ and obtains a polynomial relation just like the D–H model, but remains more nonlinearity terms of σ and the magnetoelastic coupling terms concerning quadratic terms of M, i.e.,

$$G(\sigma, M) = \frac{1}{2} \frac{\partial^2 G}{\partial \sigma^2} \sigma^2 + \frac{1}{3!} \frac{\partial^3 G}{\partial \sigma^3} \sigma^3 + \frac{1}{4!} \frac{\partial^4 G}{\partial \sigma^4} \sigma^4 + \cdots + \frac{3}{3!} \frac{\partial^3 G}{\partial \sigma \partial M^2} \sigma M^2 + \frac{6}{4!} \frac{\partial^4 G}{\partial \sigma^2 \partial M^2} \sigma^2 M^2 + \cdots$$
$$+ \frac{1}{2} \frac{\partial^2 G}{\partial M^2} M^2 + \frac{1}{4!} \frac{\partial^4 G}{\partial M^4} M^4 + \cdots \tag{1}$$

In the above Taylor series expansion of the function $G(\sigma, M)$, some terms, such as the constant term $G_0 = G(0,0)$ and the partial derivatives $\frac{\partial G}{\partial \sigma}$ and $\frac{\partial G}{\partial M}$ are neglected since they do not make any contribution to strain ε and magnetic field H at the reference point $(\sigma, M) = (0,0)$. Moreover, all the odd order terms of M are not listed in Eq. (1) because the magnetic field H is always an odd function of the magnetization M. For the experimental results by Clark (1980), the terms which describe the magnetoelastic coupling property hold only quadratic terms of M, i.e., σM^2, $\sigma^2 M^2$ and so on.

Considering the following thermodynamic relations:

$$\varepsilon = -\frac{\partial G}{\partial \sigma}, \qquad \mu_0 H = \frac{\partial G}{\partial M} \tag{2}$$

we can get

$$\varepsilon = -\frac{\partial^2 G}{\partial \sigma^2} \sigma - \frac{1}{2} \frac{\partial^3 G}{\partial \sigma^3} \sigma^2 - \frac{1}{3!} \frac{\partial^4 G}{\partial \sigma^4} \sigma^3 - \cdots$$
$$- \frac{1}{2} \left(\frac{\partial^3 G}{\partial \sigma \partial M^2} + \frac{\partial^4 G}{\partial \sigma^2 \partial M^2} \sigma + \cdots \right) M^2 \tag{3a}$$

$$\mu_0 H = \frac{\partial^2 G}{\partial M^2} M + \frac{1}{3!} \frac{\partial^4 G}{\partial M^4} M^3 + \cdots$$
$$+ \left(\frac{\partial^3 G}{\partial \sigma \partial M^2} \sigma + \frac{1}{2} \frac{\partial^4 G}{\partial \sigma^2 \partial M^2} \sigma^2 + \cdots \right) M \tag{3b}$$

where the strain exhibited in Eq. (3a) can be divided into the elastic strain, which depends only on stress σ, and the magnetostrictive strain $\lambda(M, \sigma)$, which depends on both stress σ and magnetization M and also the elastic strain can be divided into a linear part $\frac{\sigma}{E_s}$, which is independent on the magnetic domain movement, and a nonlinear part $\lambda_0(\sigma)$, which is dependent on the magnetic domain movement, where E_s is called the intrinsic (or saturation) Young's modulus (i.e., the value of Young's modulus when the magnetization approaches saturation). When the magnetization approaches to saturation the maximum magnetostrictive strain $\lambda_{max}(\sigma)$ under a given pre-stress σ should be the difference between the saturation magnetostrictive coefficient λ_s and the nonlinear elastic strain part $\lambda_0(\sigma)$, that is,

$$\lambda_{max}(\sigma) = \lambda_s - \lambda_0(\sigma) \tag{4}$$

Thus Eq. (3a) can be expressed in the following form:

$$\varepsilon = \frac{\sigma}{E_s} + \lambda_0(\sigma) + \frac{\lambda_s - \lambda_0(\sigma)}{M_s^2} M^2 \tag{5a}$$

The terms independent of stress in Eq. (3b) express the relation between magnetization M and magnetic field H of a mechanically unloaded Terfenol-D rod, which is nonlinear and has a saturation trend. A

nonlinear function $f(x)$, i.e., $M = m_s f(kH)$ is used to describe it. Then, considering the relation of coupled terms in Eqs. (3b) and (3a), Eq. (3b) can be finally rewritten as

$$H = \frac{1}{k} f^{-1}\left(\frac{M}{M_s}\right) - \frac{2(\lambda_s \sigma - \Lambda_0(\sigma))}{\mu_0 M_s^2} M \tag{5b}$$

where $\Lambda_0(\sigma) = \int_0^\sigma \lambda_0(\sigma)\,\mathrm{d}\sigma$ is the primary function of $\lambda_0(\sigma)$.

The hyperbolic tangent function $\tanh(x)$ is employed to approach to the nonlinear strain $\lambda_0(\sigma)$ and the function $f(x)$ can be chosen as the Langevin function $f(x) = \coth(x) - 1/x$. It can give a better simulation of the magnetization curve than the function $f(x) = \tanh(x)$ chosen by the D–H model, since it is based on the Boltzmann statistics and has a clear physical background. Thus, the constitutive relation shown in Eqs. (5a) and (5b) can be expressed as

$$\varepsilon = \frac{\sigma}{E_s} + \begin{cases} \lambda_s \tanh\left(\dfrac{\sigma}{\sigma_s}\right) + \left[1 - \tanh\left(\dfrac{\sigma}{\sigma_s}\right)\right]\dfrac{\lambda_s}{M_s^2}M^2 & \dfrac{\sigma}{\sigma_s} \geqslant 0 \\[2ex] \dfrac{\lambda_s}{2}\tanh\left(\dfrac{2\sigma}{\sigma_s}\right) + \left[1 - \dfrac{1}{2}\tan h\left(\dfrac{2\sigma}{\sigma_s}\right)\right]\dfrac{\lambda_s}{M_s^2}M^2 & \dfrac{\sigma}{\sigma_s} < 0 \end{cases} \tag{6a}$$

$$H = \frac{1}{k} f^{-1}\left(\frac{M}{M_s}\right) - \begin{cases} 2\left\{\sigma - \sigma_s \ln\left[\cos h\left(\dfrac{\sigma}{\sigma_s}\right)\right]\right\}\dfrac{\lambda_s}{\mu_0 M_s^2}M & \dfrac{\sigma}{\sigma_s} \geqslant 0 \\[2ex] 2\left\{\sigma - \dfrac{\sigma_s}{4}\ln\left[\cosh\left(\dfrac{2\sigma}{\sigma_s}\right)\right]\right\}\dfrac{\lambda_s}{\mu_0 M_s^2}M & \dfrac{\sigma}{\sigma_s} < 0 \end{cases} \tag{6b}$$

where $\mu_0 = 4\pi \times 10^{-7}$ H/m is the vacuum permeability, $k = 3\chi_m/M_s$ is the relaxation factor, χ_m is the magnetic susceptibility in the initial linear region, M_s is the saturation magnetization, σ_s is the stress value satisfying $\lambda_0(\sigma) = \lambda_s$ if the function $\lambda_0(\sigma)$ is simplified as a straight line and σ_s can be got based on the expression $\lambda_s = \sigma_s(1/E_0 - 1/E_s)$ after the intrinsic (or saturation) Young's modulus E_s, the initial Young's modulus E_0 and the saturation magnetostrictive coefficient λ_s have been measured. The one-dimensional constitutive relation shown by Eq. (6) is coupled and nonlinear. It is suitable for either a compressive pre-stress or a tensile one applied on the rod and the model can be used conveniently in practice since only five parameters involved in Eqs. (6a) and (6b). Those are K, E_s, M_s, λ_s, σ_s (or E_0) and they are also easy to be measured in experiments.

The D–H model (Duenas et al., 1996), which is still a coupled and nonlinear, is exhibited here for comparing with the new model

$$\varepsilon = \frac{\sigma}{E} + \frac{\lambda_s}{M_s^2}M^2 \tag{7a}$$

$$H = \frac{1}{k}\tanh^{-1}\left(\frac{M}{M_s}\right) - \frac{2\lambda_s \sigma}{\mu_0 M_s^2}M \tag{7b}$$

where the relaxation factor is $k = \chi_m/M_s$. It is obvious that Young's modulus is a constant since the relation between stress and strain is linear described by the D–H model when $M = 0$. However, the corresponding relation in Eq. (6) is still nonlinear at the time and Young's modulus should be variable with stress, i.e., the new model can describe the ΔE effect. Later, the numerical results show that the new model can also describe the reversal phenomena of magnetostrictive curve under high field, which the D–H model cannot do.

3. The numerical simulation of dynamic response on Terfenol-D rods

Terfenol-D rod, as the main element of actuator, generally works in the state of resonance for large dynamic strain in order to damp large amplitude. It is subjected to compress pre-stress, magnetic bias field

and the exciting field along the axial direction and can be looked as a fixed–free elastic rod applied compressive pre-stress P at the free end of rod. The harmonic magnetic field distributed uniformly along the axial direction of rod is $H = H_0 + H_1 \sin(2\pi f t)$, where H_0 is the magnetic bias field, H_1 is the amplitude of excitation field and f is the frequency of excitation field. Then the governing equation of longitudinal vibration on rod is expressed as

$$\frac{\partial \sigma_x}{\partial x} = \rho \frac{\partial^2 u}{\partial t^2} + \mu \frac{\partial u}{\partial t} \tag{8}$$

where ρ is the density, μ is the damping coefficient. The principle of virtual displacement is expressed as

$$\int_0^l A \delta \varepsilon_x \sigma_x \, \mathrm{d}x = \delta W_{\text{ext}} = \delta \bar{u} \times P_j - \int_0^l A \left(\delta u \rho \frac{\partial^2 u}{\partial t^2} + \delta u \mu \frac{\partial u}{\partial t} \right) \mathrm{d}x \tag{9}$$

where δW_{ext} is the virtual work of external force, $\bar{u}$ is the longitudinal displacement at the free end of rod, P_j is the external applied load at the free end of rod, u and ε_x are respectively the longitudinal displacement and longitudinal strain of rod, A is the cross-sectional area of the rod. Dividing the rod with 10 elements, the element displacement $u(x)$ can be expressed in the following form by the Lagrange interpolation polynomial, i.e.,

$$u = \boldsymbol{N} \boldsymbol{a}^e \tag{10}$$

where $\boldsymbol{a}^e$ is the displacement vector of element nodes. Substituting geometrical equation $\varepsilon_x = \frac{\mathrm{d}u}{\mathrm{d}x}$ and the constitutive relations, i.e., Eqs. (6a) and (6b) into Eq. (9), the finite element equation can be got

$$\boldsymbol{M} \ddot{\boldsymbol{a}}(t) + \boldsymbol{C} \dot{\boldsymbol{a}}(t) + \boldsymbol{K} \boldsymbol{a}(t) = \boldsymbol{Q}(t) \tag{11}$$

where $\ddot{\boldsymbol{a}}(t)$, $\dot{\boldsymbol{a}}(t)$ and $\boldsymbol{a}(t)$ are respectively the acceleration vector, velocity vector and displacement vector of node, $\boldsymbol{M}$, $\boldsymbol{C}$, $\boldsymbol{K}$ and $\boldsymbol{Q}(t)$ are respectively the mass matrix, the damping matrix, the stiffness matrix and the load array. The Rayleigh damping should be used where $\boldsymbol{C}$ is looked as linear combination of $\boldsymbol{M}$ and $\boldsymbol{K}$ and $\boldsymbol{M}$, $\boldsymbol{K}$ and $\boldsymbol{Q}(t)$ can be integrated, respectively, by cell matrix and cell array of them which are expressed as

$$\boldsymbol{M}^e = \int_0^l A \rho \boldsymbol{N}^{\mathrm{T}} \boldsymbol{N} \, \mathrm{d}x, \quad \boldsymbol{K}^e = \int_0^l A \frac{\mathrm{d}\boldsymbol{N}^{\mathrm{T}}}{\mathrm{d}x} E(\sigma_x) \frac{\mathrm{d}\boldsymbol{N}}{\mathrm{d}x} \, \mathrm{d}x$$

$$\boldsymbol{Q}^e = \int_0^l A \frac{\mathrm{d}\boldsymbol{N}^{\mathrm{T}}}{\mathrm{d}x} E(\sigma_x) \lambda(\sigma_x, H) \mathrm{d}x + P_j, \quad \begin{cases} p_j \neq 0, j = ne \\ P_j = 0, j \neq ne \end{cases} \tag{12}$$

where ne is the node number at the free end of rod, $E(\sigma_x)$ is defined as $E(\sigma_x) = \sigma_x/\varepsilon_0$, and $\varepsilon_0 = \frac{\sigma_x}{E_s} + \lambda_0(\sigma_x)$ is the strain when magnetization is zero, i.e., the former two terms in Eq. (6a). Considering Eq. (6b), the term $\frac{\lambda_s - \lambda_0(\sigma_x)}{M_s^2} M^2$, i.e., the last term in Eq. (6a) can be expressed as $\lambda(\sigma_x, H)$ which is the magnetostrictive strain when magnetization is not zero.

Eq. (11) can be expressed in the following form based on Newmark method

$$\boldsymbol{M} \ddot{\boldsymbol{a}}_{t+\Delta t} + \boldsymbol{C} \dot{\boldsymbol{a}}_{t+\Delta t} + \boldsymbol{K} \boldsymbol{a}_{t+\Delta t} = \boldsymbol{Q}_{t+\Delta t} \tag{13}$$

where

$$\dot{\boldsymbol{a}}_{t+\Delta t} = \dot{\boldsymbol{a}}_t + [(1-\delta)\ddot{\boldsymbol{a}}_t + \delta \ddot{\boldsymbol{a}}_{t+\Delta t}]\Delta t \tag{14}$$

$$\boldsymbol{a}_{t+\Delta t} = \boldsymbol{a}_t + \dot{\boldsymbol{a}}_t \Delta t + \left[\left(\frac{1}{2} - \alpha \right) \ddot{\boldsymbol{a}}_t + \alpha \ddot{\boldsymbol{a}}_{t+\Delta t} \right] \Delta t^2 \tag{15}$$

The following expression can be got by Eq. (15):

$$\ddot{\boldsymbol{a}}_{t+\Delta t} = \frac{1}{\alpha \Delta t^2} (\boldsymbol{a}_{t+\Delta t} - \boldsymbol{a}_t) - \frac{1}{\alpha \Delta t} \dot{\boldsymbol{a}}_t - \left(\frac{1}{2\alpha} - 1 \right) \ddot{\boldsymbol{a}}_t \tag{16}$$

Substituting Eq. (16) into Eq. (14) and considering Eq. (16), Eq. (13) can finally be rewritten in the following form:

$$\left(K + \frac{1}{\alpha\Delta t^2}M + \frac{\delta}{\alpha\Delta t}C\right)a_{t+\Delta t} = Q_{t+\Delta t} + M\left[\frac{1}{\alpha\Delta t^2}a_t + \frac{1}{\alpha\Delta t}\dot{a}_t + \left(\frac{1}{2\alpha}-1\right)\ddot{a}_t\right]$$
$$+ C\left[\frac{\delta}{\alpha\Delta t}a_t + \left(\frac{\delta}{\alpha}-1\right)\dot{a}_t + \left(\frac{\delta}{2\alpha}-1\right)\Delta t\ddot{a}_t\right] \tag{17}$$

Thus, the $a_{t+\Delta t}$ can be got based on a_t, $\dot{a}_t$, $\ddot{a}_t$, where $\delta = 0.5$, $\alpha = 0.25(0.5 + \delta)^2$.

The relation between stress and strain of magnetostrictive material is nonlinear. Young's modulus $E(\sigma_x)$ and the magnetostrictive strain $\lambda(\sigma_x, H)$ all relate to stress σ_x when the external magnetic field is given. The iteration process should be used for calculating $E(\sigma_x)$ and $\lambda(\sigma_x, H)$ in each time step and the flow of procedure is described as

(1) Input all the initial conditions such as the displacement a_0, the velocity $\dot{a}_0$, the acceleration $\ddot{a}_0$ and the initial stress σ_{0i} at $t = 0$.
(2) The mass matrix M, the damping matrix C and the stiffness matrix K can be integrated based on Eq. (12), where $\sigma_x = \sigma_{0i}$ in the stiffness matrix K at the moment. The time step is chosen as $\Delta t = 4 \times 10^{-6}$. The constants such as $c_0 = \frac{1}{\alpha\Delta t^2}$, $c_1 = \frac{\delta}{\alpha\Delta t}$, $c_2 = \frac{1}{\alpha\Delta t}$, $c_3 = \frac{1}{2\alpha} - 1$, $c_4 = \frac{\delta}{\alpha} - 1$, $c_5 = \frac{\Delta t}{2}\left(\frac{\delta}{\alpha} - 2\right)$, $c_6 = \Delta t(1 - \delta)$, $c_7 = \delta\Delta t$ are calculated.
(3) Calculate the effective stiffness matrix by $\widehat{K} = K + c_0 M + c_1 C$.
(4) The load array at the moment $t + \Delta t$, i.e., $Q_{t+\Delta t}$ can be integrated based on Eq. (12), and then the effective load array at the moment can be calculated by $\widehat{Q}_{t+\Delta t} = Q_{t+\Delta t} + M(c_0 a_t + c_2\dot{a}_t + c_3\ddot{a}_t) + C(c_1 a_t + c_4\dot{a}_t + c_5\ddot{a}_t)$, where $\sigma_x = \sigma_{0i}$ and $H = H_{t+\Delta t}$ in the load array $Q_{t+\Delta t}$ at the moment.
(5) Calculate the displacement at the moment $t + \Delta t$, i.e., $a_{t+\Delta t}$ by $\widehat{K}a_{t+\Delta t} = \widehat{Q}_{t+\Delta t}$, then the acceleration $\ddot{a}_{t+\Delta t}$ and the velocity $\dot{a}_{t+\Delta t}$ can be calculated, respectively, by expressions $\ddot{a}_{t+\Delta t} = c_0(a_{t+\Delta t} - a_t) - c_2\dot{a}_t - c_3\ddot{a}_t$ and $\dot{a}_{t+\Delta t} = \dot{a}_t + c_6\ddot{a}_t + c_7\ddot{a}_{t+\Delta t}$. The iteration process should be used in calculating the stiffness matrix K and the load array $Q_{t+\Delta t}$ for the stress σ_x. The strain at the moment $t + \Delta t$, i.e., $\varepsilon_{t+\Delta t}$ can be calculated by $\varepsilon_x = \frac{du}{dx}$ when u is replaced by $a_{t+\Delta t}$, thus a modified stress $\sigma_{0(i+1)} = E_i(\sigma_{0i})\varepsilon_{0(i+1)}$ at the moment can be calculated by the expression $\varepsilon_{0(i+1)} = \varepsilon_{t+\Delta t} - \lambda(\sigma_{0i}, H_{t+\Delta t})$. If the precision condition, i.e., $\|\Delta\sigma_0\| < \delta$ ($\delta = 1 \times 10^{-6}$) cannot be satisfied, σ_{0i} should be replaced by $\sigma_{0(i+1)}$ and the program should go to step (2) until it satisfies the precision condition; otherwise $\sigma_{0(i+1)}$ is the true stress of the rod at the moment. Replacing σ_{0i} by $\sigma_{0(i+1)}$, t by $t + \Delta t$ and going to step (2), the next step is going on.

Repeating the steps (2)–(4), the deflection of the rod at any moment are t reached.

4. Results analysis

First, a comparison about magnetostrictive strain versus magnetic field for Terfenol-D rod between the D–H model and the new model is made which verifies the new model's validity on describing the coupled mechanics-magneto property of magnetostrictive material.

As shown in Fig. 3, the magnetostrictive strains predicted by the D–H model reach the same value in the region of the high field. It means the D–H model fails to simulate the reversal phenomena shown in Fig. 1. Fig. 4 is the curves of magnetostrictive strain versus magnetic field for Terfenol-D rod under different compressive pre-stress based on the new model. It can be seen that the magnetostrictive strain increases with increasing magnetic field for a given pre-stress and decreases with increasing compressive pre-stress for
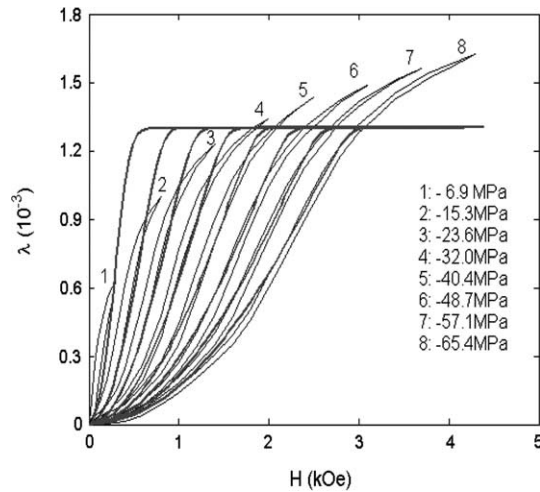
Fig. 3. The curves of magnetostrictive strain versus magnetic field (hysteresis loops: experimental (Moffet et al., 1991); solid lines: the D–H model).
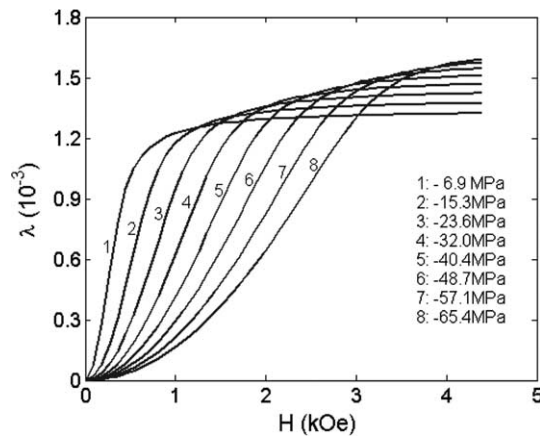

Fig. 4. The curves of magnetostrictive strain versus magnetic field (the model in this paper).

low or moderate magnetic field. When the applied magnetic field is high or near saturation, the magnetostrictive strain of the rod will reach different saturation values for different pre-stresses. As shown in Fig. 4, the maximum magnetostrictive strain of a Terfenol-D rod increases with increasing compressive pre-stresses under high field, which describes the reversal phenomena mentioned in this paper. These results predicted by the new model are coincident with the experimental phenomena (Butler, 1988; Moffet et al., 1991). It shows that the model is better than the D–H model to describe the coupled mechanics-magneto property of magnetostrictive material under different compressive pre-stress and different external magnetic field.

Then, the numerical simulation of dynamic response on Terfenol-D actuator is made according to the new model and the numerical procedure of the paper. The results are compared with those by the D–H models. The length of the Terfenol-D rod is 114.5 mm, and the other physical parameters are, respectively, taken as $\rho = 9130 \text{ kg/m}^3$, $\lambda_s = 1300$ ppm, $\mu_0 M_s = 0.8$ T, $\chi_m = 80$, $E_s = 110$ Gpa, $\sigma_s = 200$ Mpa. And the

element number of the rod and the time step are, respectively, taken as 10 and $\Delta_t = 4 \times 10^{-6}$ s in our calculation. The numerical tests show that the element number of the rod and the time step are enough for stability.

Fig. 5(a) shows the curves of resonance frequency versus the magnetic bias field for a given pre-stress based on the D–H model and the new model, respectively. It can be seen that there is a notable difference between different models under high field. The resonance frequency predicted by the D–H model is a constant, which does not change with the external magnetic bias field. But the corresponding result predicted by the new model is different. It shows that the resonance frequency increases nonlinearly with increasing magnetic bias field, which is coincident with the experimental phenomena shown in Fig. 2. It means that the model is also better than the D–H model to describe the law between resonance frequency and the magnetic bias field under high field. Moreover, numerical results by the new model show that the resonance amplitude decreases with increasing magnetic bias field under high field, which is shown in Fig. 5(b). It can be explained that the magnetostrictive strain described by the new model approaches the saturation gradually and the slope of the curves shown in Fig. 4 decreases gradually with increasing magnetic field under high field, thus, the deformation induced by the exciting field H_1 decreases with increasing magnetic bias field H_0 at the time. The corresponding resonance amplitude prescribed by the D–H model is zero under high field, which is also shown in Fig. 5(b). This is due to the fact that the maximum magnetostrictive strain described by the D–H model is a constant and the slope of curves shown in Fig. 3 is zero at the time, thus, the deformation induced by the exciting field H_1 is zero under high magnetic bias field H_0 and corresponding resonance amplitude is zero at the time.

Fig. 6 is the curves of resonance frequency versus the compressive pre-stress for a given magnetic bias field based on the D–H model and the new model, respectively. It can be seen that the resonance frequency described by the new model increases nonlinearly with increasing compressive pre-stress when the magnetic bias field and the exciting field are, respectively, 0 Oe and 100 Oe. However, the corresponding resonance frequency described by the D–H model is a constant and does not change with the pre-stress. It because that Young's modulus prescribed by the D–H model is a constant, yet the relation between Young's modulus and the stress prescribed by the new model is nonlinear at the time.

Fig. 7 is the response curves of amplitude versus time for the Terfenol-D rod prescribed by the new model when external magnetic field approaches the saturation. The ultraharmonic resonance phenomenon
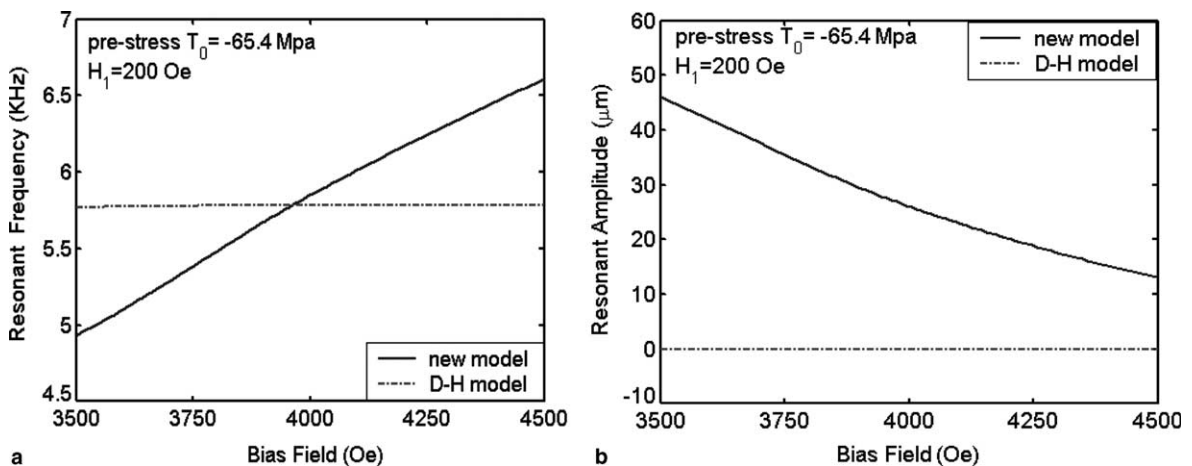

Fig. 5. (a) The curves of resonance frequency versus the magnetic bias filed. (b) The curves of resonance amplitude versus the magnetic bias filed.
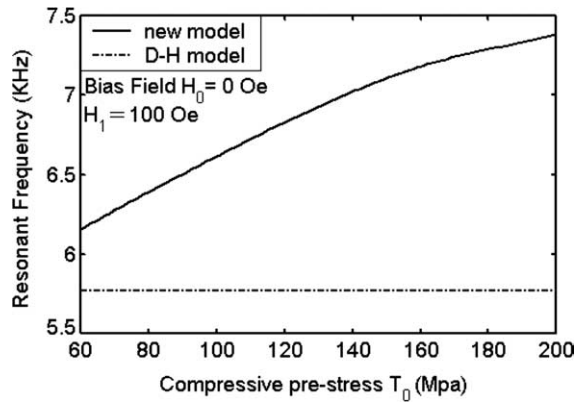
Fig. 6. The curves of resonance frequency versus the compressive pre-stress.
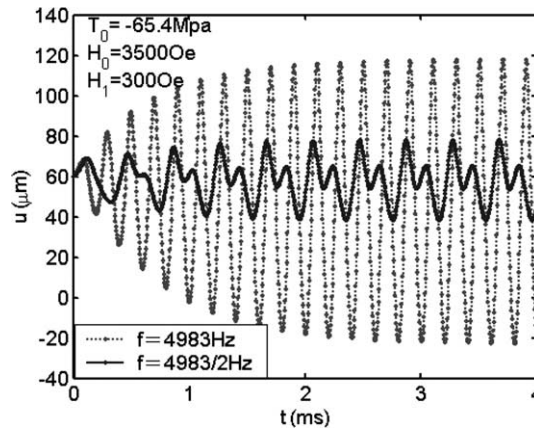

Fig. 7. The response curves of amplitude versus time.

is shown in Fig. 7, which is the character of nonlinear vibration, where the resonance frequency is 4983 Hz. However, the D–H model cannot prescribe the phenomena at all since constitutive relation prescribed by the D–H model is linear at the time. As shown in Fig. 3, the magnetostrictive strain prescribed by the D–H model is a constant when magnetic field and pre-stress are, respectively, 3.5 kOe and -65.4 MPa, i.e., the constitutive relation is $\varepsilon \frac{\sigma}{E} +$ constant in Eq. (7a) at the time.

Based on above analysis, the new model is better than the D–H model to describe the magnetostrictive strain in different compressive pre-stress and different magnetic field. Especially under the high field, it can describe the reversal phenomena, which the D–H model cannot do. Furthermore, the new model can describe the ΔE effect more accurately, which makes it more accurately in describing the drift of resonance hump of the Terfenol-D actuator. In practice the law of the drift is important for getting the expectant resonance frequency or resonance amplitude by changing the magnetic bias field and pre-stress and also the model presented in this paper can describe the ultraharmonic resonance phenomena under high field, which is the character of nonlinear vibration. All of the results are due to the intrinsic advantage of the new model in describing the coupled mechanics-magneto property of Terfenol-D rod.

Acknowledgement

References

Butler, J.L., 1988. Application Manual for Design of Etrema Terfenol-D Magnetostrictive Transducers. Edge Technologies, Inc., Ames.

Carman, G.P., Mitrovic, M., 1995. Nonlinear constitutive relation for magnetostrictive materials with applications to 1-D problems. Journal of Intelligent Material Systems and Structures 6, 673–683.

Clark, A.E., 1980. Magnetostrictive rare earth-Fe_2 compounds. In: Wohlfarth, E.P. (Ed.), Ferromagnetic Materials, vol. 1. North-Holland Publishing Co., Amsterdam, pp. 531–589.

Duenas, T., Hsu, L., Carman, G.P., 1996. Magnetostrictive composite material systems analytical/experimental. In: Materials Research Society Symposium, Advances in Materials for Smart Systems—Fundamental and Applications (Invited paper), Boston, 1996.

Engdahl, G., Svensson, L., 1988. Simulation of the magentostrictive performance of Terfenol-D in mechanical devices. Journal of Applied Physics 63 (8), 3924–3926.

Jenner, A.G., Greenough, R.D., Allwood, D., Wilkinson, A.J., 1994. Control of Terfenol-D under load. Journal of Applied Physics 76 (10), 7160–7162.

Kvarnsjö, L., Engdahl, G., 1991a. Nonlinear 2-D transient modeling of Terfenol-D rods. IEEE Transactions of Magnetics 27 (6), 5349–5351.

Kvarnsjö, L., Engdahl, G., 1991b. Examination of the interaction between eddy currents and magnetoelasticity in Terfenol-D. Journal of Applied Physics 69 (8), 5783–5785.

Mahapatra, D.R., Gopalakrishnan, S., Balachandran, B., 2001. Active feedback control of multiple waves in helicopter gearbox support struts. Smart Materials and Structures 10, 1046–1058.

Moffet, M.B., Clark, A.E., Fogle, M.W., Linberg, J., Teter, J.P., McLaughlin, E.A., 1991. Characterization of Terfenol-D for magnetostrictive transducers. Journal of the Acoustical Society of America 89 (3), 1448–1455.

Pelinescu, I., Balachandran, B., 2001. Analytical study of active control of wave transmission through cylindrical struts [in helicopters]. Smart Materials and Structures 10 (1), 121–136.

Rodtlett, P.A., Eaton, S.J., Gore, J., Metheringham, W.J., Jenner, A.G., 2001. High power low frequency magnetostrictive actuation for anti-vibration applications. Sensors and Actuators A 91, 133–136.

Savage, H.T., Clark, A.E., Powers, J.H., 1975. Magnetomechanical coupling and ΔE effect in highly magnetostrictive rare earth-Fe_2 compounds. IEEE Transactions on Magnetics 11 (5), 1355–1357.

Wan, Y.P., Fang, D.N., Hwang, K.C., 2003. Non-linear constitutive relations for magnetostrictive materials. International Journal of Non-Linear Mechanics 38, 1053–1065.

Zhou, Y.H., Miya, K., 1999. A theoretical predication of increase of natural frequency to ferromagnetic plates under in-plane magnetic fields. Journal of Sound and Vibration 222 (1), 49–64.

Zhou, Y.H., Tzou, H.S., 2000. Active control of nonlinear piezoelectric circular spherical shells. International Journal of Solids and Structures 37, 1663–1677.